Fast reconstruction of multiphase microstructures based on statistical descriptors

DongDong Chen,[1] Zhi Xu,[2,*] XiaoRui Wang,[1] HongJie He,[1] ZhongZhou Du,[1] and JiaoFen Nan[1]

[1]*School of Computer and Communication Engineering, Zhengzhou University of Light Industry, Zhengzhou, 450000, China*

[2]*Guangxi Key Laboratory of Images and Graphics Intelligent Processing, Guilin University of Electronics Technology, Guilin, 541004, China*

(Received 18 February 2022; accepted 6 April 2022; published 3 May 2022)

In this paper, we propose a hierarchical simulated annealing of erosion method (HSAE) to improve the computational efficiency of multiphase microstructure reconstruction, whose computational efficiency can be improved by an order of magnitude. Reconstruction of the two-dimensional (2D) and three-dimensional (3D) multiphase microstructures (pore, grain, and clay) based on simulated annealing (SA) and HSAE are performed. In the reconstruction of multiphase microstructure with HSAE and SA, three independent two-point correlation functions are chosen as the morphological information descriptors. The two-point cluster function which contains significant high-order statistical information is used to verify the reconstruction results. From the analysis of 2D reconstruction, it can find that the proposed HSAE technique not only improves the quality of reconstruction, but also improves the computational efficiency. The reconstructions of our proposed method are still imperfect. This is because the used two-point correlation functions contain insufficient information. For the 3D reconstruction, the two-point correlation functions of the 3D generation are in excellent agreement with those of the original 2D image, which illustrates that our proposed method is effective for the reconstruction of 3D microstructure. The comparison of the energy vs computational time between the SA and HSAE methods shows that our presented method is an order of magnitude faster than the SA method. That is because only some of the pixels in the overall hierarchy need to be considered for sampling.

DOI: 10.1103/PhysRevE.105.055301

I. INTRODUCTION

The physical properties of porous material (such as mechanical properties, capillary properties, electrical conductivity, and permeability) are closely related to their three-dimensional (3D) structure, which is composed of a solid material skeleton and many crowded micropores [1–11]. It is of great significance to understand and model the internal structure of porous material [12–15]. There are two methods of reproducing the 3D microstructure of a porous material. The first method is based on instruments such as the scanning electron microscope (SEM) and computed tomography (CT), and the focused ion beam (FIB). This method can directly and accurately obtain the real 3D data of porous material, but in many cases only the two-dimensional (2D) section of the porous material can be obtained. Therefore, it is of great value to reconstruct the 3D microstructure of porous material from a 2D image in such case.

In the past few decades, a variety of reconstruction methods have been developed using the limited morphological information contained in 2D images [16–40]. A widely used reconstruction method is based on statistical feature functions. Two common methods based on statistical reconstruction have been actively adopted: the Gaussian random field method (GRF) [25–27] and the simulated annealing method (SA) [28–38]. The first method is based on the conditioning and truncation of Gaussian random fields: Based on the given two-point correlation function, the field correlation function is first constructed. Then, the Gaussian random field, whose horizontal cutting results are correlated with the target two-point correlation function, is generated from the field correlation function. Although a variety of microstructures can be generated with a two-point correlation function using this method, it is difficult to extend to other correlation functions and anisotropic multiphase media.

The simulated annealing method (also called the Yeong-Torquato procedure) is treated as an energy minimization problem, whereby one tries to minimize the energy between the reference and reconstructed microstructure. This method is model independent and can flexibly combine multiple statistical descriptors to more effectively describe the spatial characteristics of random porous structures. In addition, this algorithm is a global optimization algorithm that minimizes the statistical feature difference between the reconstructed image and the original 2D image to generate the optimal structure.

This method has strong flexibility and universality, but due to its randomness, this approach is time consuming for the convergence of the objective function. In order to improve the convergence rate, several methods in the SA reconstruction framework [30,39,40] have been presented to improve the performance of this method. Tang *et al.* [39] proposed a pixel selection rule to speed up the reconstruction process, where the selection probability of a pixel is determined by its number of different phase neighbors (DPNs). Jiao *et al.* [30] proposed the "surface optimization" rule to improve the reconstruction speed, where pixels are divided into a low-energy subset and

*Corresponding author: xuzhi@guet.edu.cn

a high-energy subset. Only pixels in the high-energy subset are selected. Alexander *et al.* [24] proposed a hierarchical simulated annealing (HSA) method to reduce the computational cost so that more complex synthesis problems can be attempted using this method on large multiscale images. Although HSA can improve the reconstruction speed, it can magnify the reconstruction error of coarse scale during the synthesis process. With the process of the synthesis, the error of the final reconstruction is continuously enlarged. All these methods are mainly aimed at the reconstruction of a two-phase microstructure. For the reconstruction of a multiphase microstructure, the hierarchical simulated annealing of erosion method (HSAE) is proposed to improve the computational efficiency.

The rest of this paper is arranged as follows: The description of the two-point correlation function for multiphase microstructure is given in Sec. II. In Sec. III, our presented method is briefly outlined. In Sec. IV, the reconstruction of 2D structures and 3D structures based on the reference 2D images is performed, where the unconstrained two-point cluster function $C_2(r)$ is computed and compared to illustrate the advantage of our proposed method. It is noted that the presented method can reconstruct more accurate microstructure from the reference 2D image. Finally, remarks are concluded in Sec. V.

II. TWO-POINT CORRELATION FUNCTION OF MULTIPHASE MICROSTRUCTURE

The two-point correlation function (TPCF) is acquired by throwing numbers of random vectors on the microstructure, examining the number fraction of the beginning and ending of each vector ($\vec{r}$) lying in a particular phase (Fig. 1). For a three-phase microstructure, there exist three phases (phase 1, phase 2, and phase 3) with the volume fraction of each phase defined as follows:

$$\frac{V_k}{V_{\text{total}}} = v_k, \quad k \in [1, 2, 3], \tag{1}$$

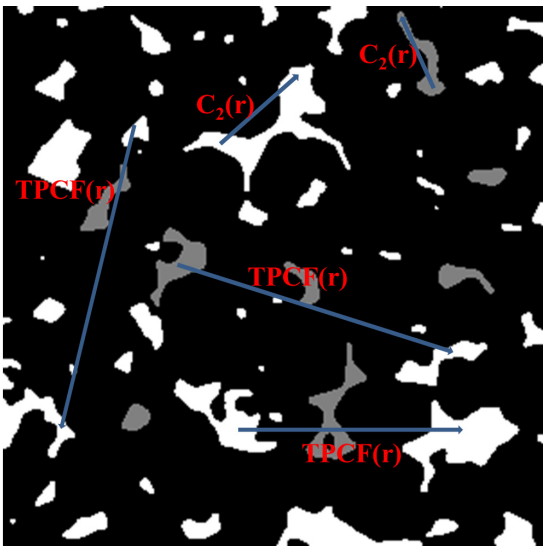

FIG. 1. Schematic illustration of different correlation functions.

where V_1, V_2, and V_3 are the volumes of three phases, respectively, and v_1, v_2, and v_3 are their corresponding volume fractions. Obviously,

$$\sum_{k=1}^{3} V_k = V_{\text{total}} \quad \text{and} \quad \sum_{k=1}^{3} v_k = 1. \tag{2}$$

If N points are randomly thrown into a given microstructure and the number of points falling into phase k is N_k, then the one-point probability function P_k can define the volume fraction through the following relation as N (the total number) is increased to infinity:

$$P_k = \left.\frac{N_k}{N}\right|_{N\to\infty} = v_k. \tag{3}$$

Now, randomly throw the vectors in a three-phase microstructure as shown in Fig. 1. Depending on the head and the tail of these vectors falling within phase 1 or phase 2 or phase 3, there will be nine different probabilities, P_{11}, $P_{12}, P_{13}, P_{21}, P_{22}, P_{23}, P_{31}, P_{32}, P_{33}$, defined as follows:

$$P_{kl}(\vec{r}) = \left.\frac{N_{kl}}{N}\right|_{N\to\infty} \{\vec{r} = \overrightarrow{r_l} - \overrightarrow{r_k}, (\overrightarrow{r_l} \in \emptyset_l) \cap (\overrightarrow{r_k} \in \emptyset_k)\}, \tag{4}$$

where N_{kl} is the number of vectors with the head in phase k and the tail in phase l. Equation (4) defines a joint probability distribution function to describe the occurrence of events constructed by two points as the head and tail of a vector when it is randomly thrown into a microstructure N number of times. The two-point probability function can be defined based on two other probability functions such that

$$P_{kl}(\vec{r}) = P\{(\overrightarrow{r_l} \in \emptyset_l)|(\overrightarrow{r_k} \in \emptyset_k)\}P\{(\overrightarrow{r_k} \in \emptyset_k)\}. \tag{5}$$

The first term on the right-hand side of Eq. (5) is a conditional probability function. Note that for very long distances $\vec{r} \to \infty$, the probability of the head point does not affect the tail point and the two points become irrelevant or statistically independent. The conditional probability function is reduced to a one-point function,

$$P(\overrightarrow{r_k} \in \emptyset_k) = P\{(\vec{r} \to \infty), (\overrightarrow{r_k} \in \emptyset_k)|(\overrightarrow{r_l} \in \emptyset_l)\}. \tag{6}$$

The two-point correlation function will then be reduced to

$$P_{kl}(\vec{r}) = P(\overrightarrow{r_l} \in \emptyset_l)P(\overrightarrow{r_k} \in \emptyset_k), \tag{7}$$

or

$$P_{kl}(\infty) = v_k v_l. \tag{8}$$

For the periodic boundary condition of the microstructure, the two-point correlation function is satisfied by the following relationship:

$$P_{kl}(\vec{r}) = P_{lk}(\vec{r}). \tag{9}$$

Due to normality conditions, a three-phase microstructure is satisfied by the following equations:

$$\sum_{k=1}^{3}\sum_{l=1}^{3} P_{kl}(\vec{r}) = 1, \tag{10}$$

$$\sum_{l=1}^{3} P_{kl}(\vec{r}) = v_k, \tag{11}$$

$$\sum_{k=1}^{3} P_{kl}(\vec{r}) = v_l. \tag{12}$$

Satisfying all three conditions for a three-phase microstructure $[k, l \in (1-3)]$, three nonlinear correlation equations can be obtained as follows:

$$P_{11} + P_{12} + P_{13} = v_{1,} \tag{13}$$

$$P_{21} + P_{22} + P_{23} = v_{2,} \tag{14}$$

$$P_{31} + P_{32} + P_{33} = v_3. \tag{15}$$

Because the probability functions are symmetric ($P_{kl} = P_{lk}$), the nine probability functions will be reduced to six independent functions, P_{11}, $P_{12}, P_{13}, P_{22}, P_{23}, P_{33}$. In the reconstruction of three-phase microstructure, only three independent probabilities need to be considered as independent variables. In this paper, P_{11}, P_{12}, and P_{22} are chosen as the three probability parameters. The other probability functions can be obtained through Eqs. (13)–(15). In all reconstructed systems, the sampling is performed in the X and Y directions in a porous medium. This sampling procedure is more accurate than that by random sampling (throwing random points into the system), because the former exhaustively incorporates the information of each pixel in the entire system.

III. RECONSTRUCTION METHOD

A. Simulated annealing

In the procedure of multiphase reconstruction, the modified Yeong-Torquato technique (SA method) is utilized, where some energy function $E(x)$ is needed. The two-point probability function which contains numbers of properties of the microstructure is chosen to express the structural information. The energy function $E(x)$ is expressed as the sum of squared differences between the reference structure and the reconstructed structure:

$$E(x) = \sum_{r}[(P_{11}(x) - P_{11})^2 + (P_{12}(x) - P_{12})^2 + (P_{22}(x) - P_{22})^2], \tag{16}$$

where P_{11}, P_{12}, P_{22}, and $P_{11}(x)$, $P_{12}(x)$, $P_{22}(x)$ are respectively expressed as the selected two-point probability function of the reference structure and the reconstructed structure.

The microstructure reconstruction, whose aim is to minimize the energy function $E(x)$, can be viewed as the optimized problem. To evolve the digitized system toward the reference medium [or, in other words, minimizing $E(x)$], the states of two arbitrarily selected pixels of different phases are interchanged. After the interchange is performed, the energy E' of the new state and the energy difference $\Delta E = E' - E$ between two successive states of the system are calculated. Then the new state is accepted with probability $P(\Delta E)$ via the Metropolis method as

$$P(\Delta E) = \begin{cases} 1, & \Delta E \leqslant 0 \\ \exp\left(-\frac{\Delta E}{T}\right), & \Delta E > 0 \end{cases}, \tag{17}$$

where T is the "temperature." The decreased rate of T is controlled by a cooling schedule which controls the system to evolve to the desired state as quickly as possible without falling into any local energy minimum. The algorithm is terminated when the number of consecutive unsuccessful phase interchanges is greater than a large number $2 \times 10^5 \geqslant 0$ or T is lower than 1.0×10^{-38}.

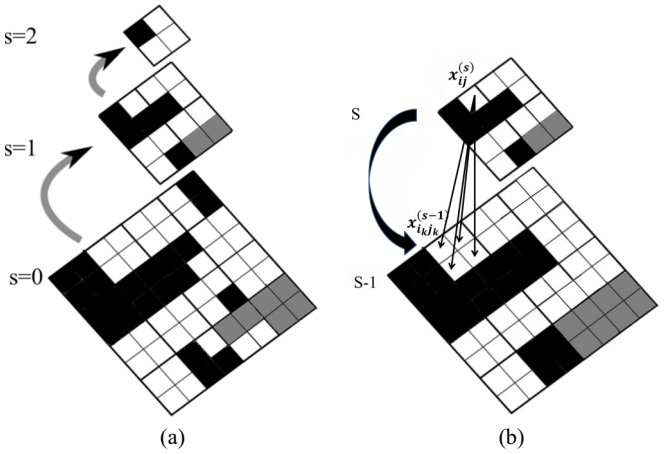

FIG. 2. The synthesis rule of reference image and the refinement rule of a reconstructed image. (a) is the synthesis rule of the reference image; (b) is the refinement rule of the reconstructed image.

B. Hierarchical annealing of erosion method

To solve the problem of slow convergence in multiphase reconstruction problems, a hierarchical annealing method is proposed. The hierarchical annealing method is initiated from reconstructing a coarse-scale image, which is then continuously refined until the desired size has been achieved. At each scale, the reconstruction is performed as an independent simulated annealing problem.

The hierarchical annealing method has two key parts: the synthesis of the reference image and the refinement of the reconstructed image shown in Fig. 2. Figure 2(a) shows the schematic of the process for synthesizing coarse reference images from the original high-resolution image, in which $x_{ij}^{(s)}$ represents an image at scale s where increasing s signifies progressively coarser scales, and $x_{ij}^{(s)}$ denotes the pixel value of $x^{(s)}$ at position ij. Let $\{i_1 j_1,\ i_2 j_2,\ i_3 j_3,\ i_4 j_4\}$ be the indices of the children of $x_{ij}^{(s+1)}$ at scale s. For a given three-phase structure, the coarser-scale representation $x_{ij}^{(s+1)}$ can be obtained from the finer-scale image $x^{(s)}$ using the following rule:

$$x_{ij}^{(s+1)} = x_{(2i)(2j)}^{s}, \quad \text{where } i \in \left(0, 1, \ldots, \frac{\text{width}}{2}\right) \text{ and } j \in \left(0, 1, \ldots, \frac{\text{height}}{2}\right). \tag{18}$$

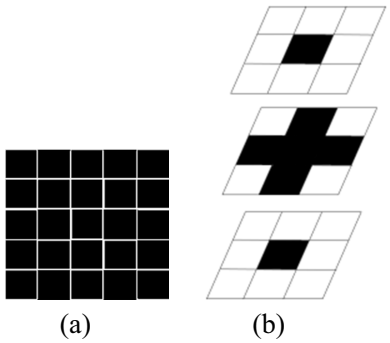

FIG. 3. Black pixels represent structural elements. (a) shows the 2D structural elements; (b) shows the 3D structural elements.

The width and height are the width and height of finer-scale image $x^{(s)}$. The coarsening of the original high-resolution target image will introduce errors in the coarse images. The coarsening will cause some information about the microstructure to be lost (leading to inaccurate reconstruction), where the lost information is located at the intersection of different phases.

Another key part of the hierarchical annealing method is the refinement of images during reconstruction. The reconstruction, starting with the coarsest scale, is performed using SA. Once a final solution of the coarsest scale is achieved, each pixel is decomposed into four new pixels (children pixels). The refinement rules are defined as follows:

$$if\ x_{ij}^{(s)} \in \{0, 128, 255\},\quad \text{then}\ x_{i_k j_k}^{(s-1)} = x_{ij}^{(s)}\ (k \in 1, 2, 3, 4). \tag{19}$$

This process is repeated until the reconstruction of zero scale is completed.

In order to avoid the information loss of the synthesized fine structure from the reconstructed structure of coarse scale, the hierarchical simulated annealing of erosion method is proposed. The key idea of our proposed method is that the reconstructed structure of coarse scale is first synthesized as the fine structure; then the fine structure is corroded by structural elements. The structural elements used for 2D and 3D reconstruction in this paper are shown in Fig. 3. The synthesized fine structure loses some information compared with the reference image, where the lost information is also located at the intersection of different phases. The corrosion operation can make the intersection region of different phases in the synthesized fine structure as an unstable state to participate in the reconstruction, which can revise the error of the reconstructed structure. Since the nonerosion pixels as the frozen state are not allowed to be swapped, the number of pixels to be swapped is reduced. Our proposed method can improve the computational efficiency of multiphase microstructure

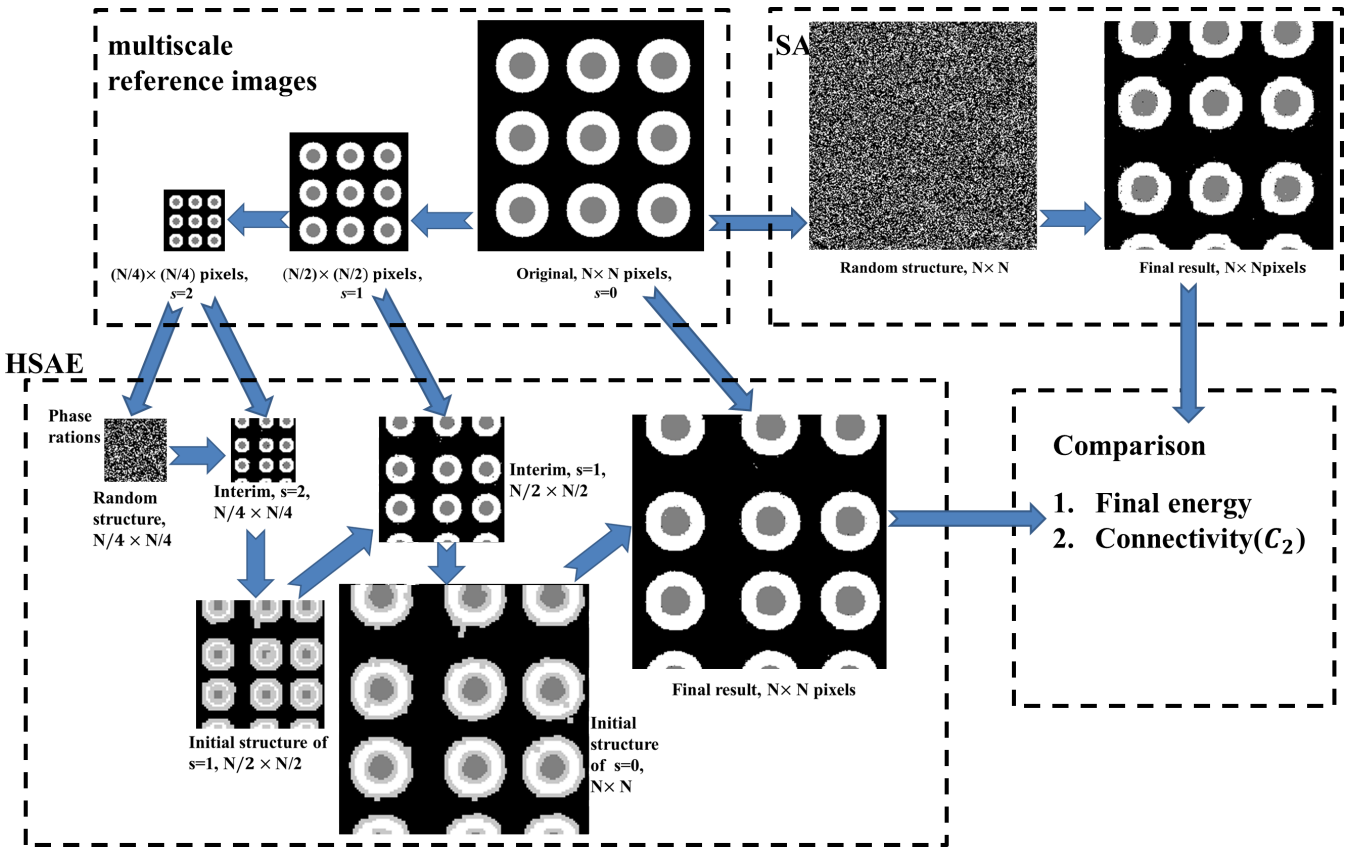

FIG. 4. The general scheme of hierarchical simulated annealing of erosion method (HSAE) and the comparison of its results against simulated annealing (SA) reconstructions based on the two-point correction functions. In the scheme, N refers to the image width and height in pixels, s is the hierarchical layer, and the gray pixels (the value is 200) are nonfrozen states. The final results for HSAE and SA are the best reconstructions for these methods among five replicas.

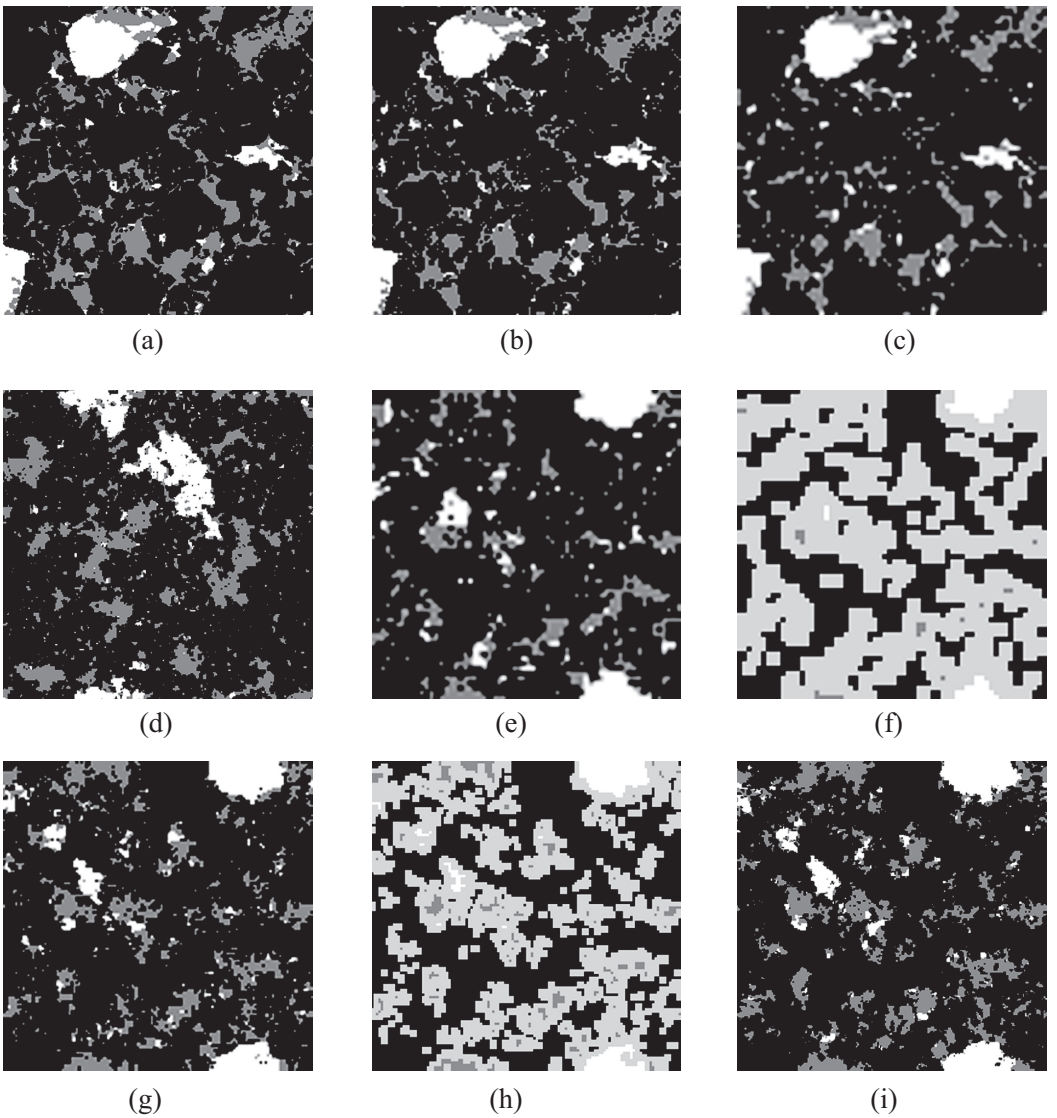

FIG. 5. (a) is the original image at a full resolution of 256 × 256. Its corresponding coarser scales are (b) 128 × 128 and (c) 64 × 64. (d) is the result of SA reconstruction. The results of the HSAE reconstruction are (e) 64 × 64, (g) 128 × 128, and (i) 256 × 256. The erosion structure as the initial structure of scale 1 and scale 0 are (f) 128 × 128 and (h) 256 × 256.

reconstruction. In the process of hierarchical reconstruction, each scale is treated as a separate annealing procedure. For the coarsest structure and the finer structure reconstruction, the temperature is chosen so that the probability p for $\Delta E \geqslant 0$ respectively equals 0.5 and 0.1. For all scale reconstruction, T is decreased according to the following cooling scheme:

$$T(k) = T(k-1)\lambda, \tag{20}$$

where k is the time step and λ is a tuning factor ($\lambda = 0.99$ for all reconstructions presented here). The periodic boundary condition was applied for statistical function calculation.

IV. DISCUSSION AND RESULTS

In this section, the 2D reconstructions of three-phase structures are first performed on SA and HSAE, respectively. Then the reconstruction method is applied to perform the 3D reconstruction of the sandstone sample. For each three-phase microstructure, five stochastic reconstructions were performed for both the SA and HSAE methods to investigate its variability. Two metrics are used to evaluate the accuracy of the SA method and the HSAE method: (1) the final reconstruction energy; (2) the error based on the two-point clustering function. The final reconstruction energy is a direct measure of the effectiveness of the stochastic reconstruction process, showing how easily the system can reach the ground state. The two-point clustering function with important higher-order statistical information is a measure of both pore connectivity and accuracy.

A. SA and HSAE performed on the 2D reconstruction of three-phase structure

In this paper, two random images with size 256 × 256 are performed on the 2D reconstruction of the three-phase structure, shown in Figs. 4 and 5. The hierarchical reconstruction of three-phase microstructures, in which each reference structure is rescaled by the coarsening rule of Eq. (18), has

TABLE I. Statistics for the best reconstructions using HSAE and SA methods for each of the original 2D images.

	Three-phase ring		Sandstone	
The best replica for the sample	SA	HSAE	SA	HSAE
Final energy [according to Eq. (16)]	1.58×10^{-4}	1.09×10^{-5}	3.56×10^{-6}	2.85×10^{-6}
Cluster error (pore phase)	8.51×10^{-5}	6.7×10^{-6}	0.000323	0.000268
Computation time (s)	679	114	268	94

three hierarchical levels. The general scheme of our proposed method is shown in Fig. 4. Similar to SA, a random mixture of pixels for the coarsest scale s is first generated according to the ration of the white, gray, and black phases of the reference structure. After T is lower than 1.0×10^{-38} or 2×10^5 consecutive unsuccessful permutations are reached, the reconstruction of the coarsest scale s is completed. Each pixel of the reconstruction is decomposed into four new pixels to move to the next hierarchical level, which is then corroded as the initial structure of the s-1 level (the corroded structure is then randomly changed to the white, gray, or black phase based on the next scale reference structure). Because each scale is treated as a separate annealing procedure, for the reconstruction of the second level $s = 1$ and the final level $s = 0$, the initial temperature is chosen so that the probability p equals 0.1 for $\Delta E \geqslant 0$ and the annealing is completed until the same criteria as for the SA method are reached.

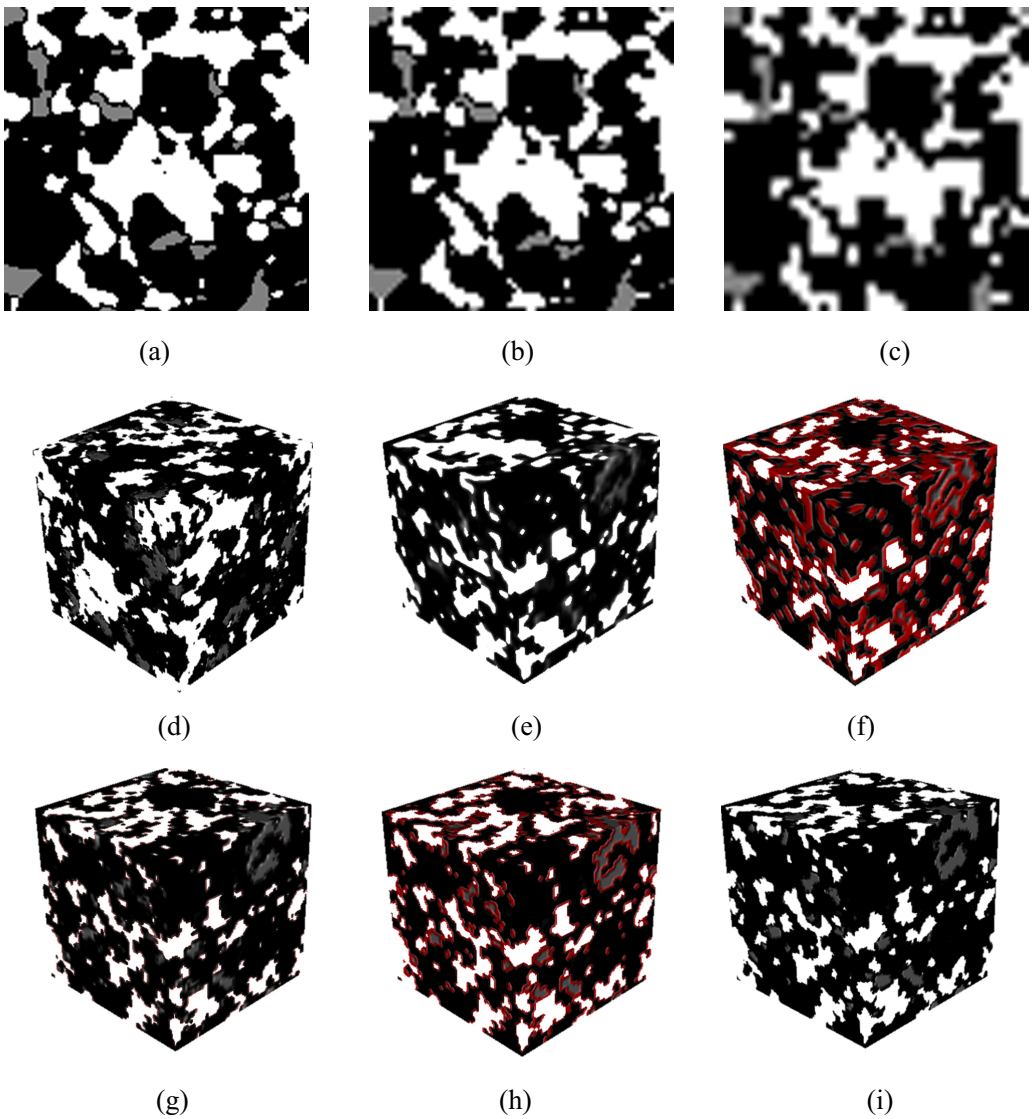

FIG. 6. (a) is the original image at a full resolution of 128 × 128. Its corresponding coarser scales are (b) 64 × 64 and (c) 32 × 32. (d) is the result of SA reconstruction. The results of the HSAE reconstruction are (e) 32 × 32 × 32, (g) 64 × 64 × 64, and (i) 128 × 128 × 128. The erosion structure as the initial structure of scale 1 and scale 0 are (f) 64 × 64 × 64 and (h) 128 × 128 × 128.

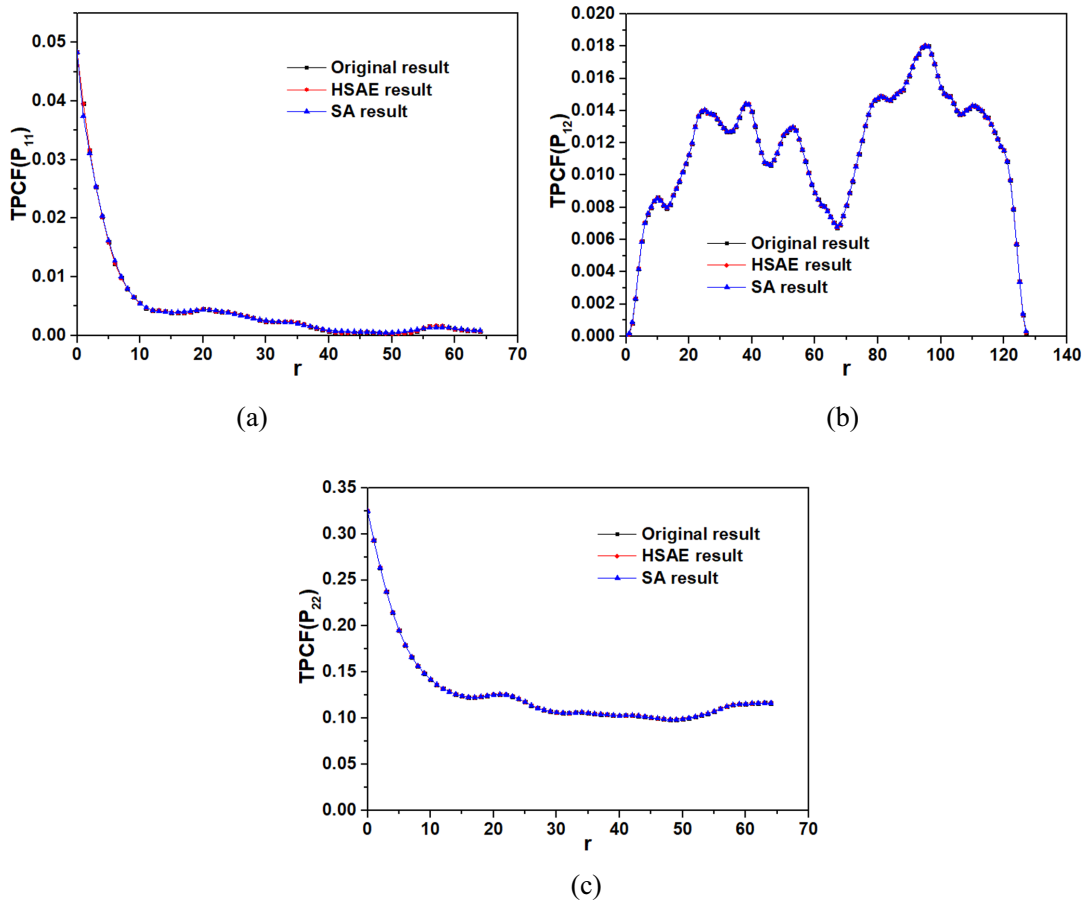

FIG. 7. Comparison diagrams of the two-point correlation function (TPCF) for the original and the reconstructed images. (a) is the two-point correlation function P_{11} for the clay phase; (b) is the two-point (clay-pore) correlation function P_{12}; (c) is the two-point correlation function P_{22} for the pore phase.

The best reconstructions of two random images based on the SA and HSAE methods are displayed in Figs. 4 and 5. The comparisons of the metrics for the reconstructions are shown in Table I. As can be seen from Table I, the HSAE reconstructions exceed the SA reconstructions in terms of the metrics used. After annealing termination, the final reconstruction energy of the HSAE method is lower, and according to the clustering function, the overall connectivity and accuracy of the HSAE method are approximately orders of magnitude better than the SA reconstruction. Because only some of the pixels are needed to participate in the finer-scale reconstruction, the reconstruction time of our proposed method is faster than that of the SA reconstruction. From Table I, it can be seen that the proposed method can not only improve the reconstruction speed but also the reconstruction accuracy. The $C_2(r)$ function of pore phase for the reconstruction of the scale $s = 2$ and the scale $s = 1$ shown in Figs. 4 and 5 is also compared to the corresponding reference microstructure. The errors for the reconstruction of the scale $s = 2$ and the scale $s = 1$ with the HSAE method are 5.17×10^{-5} and 1.26×10^{-4} shown in Fig. 4 and 7.64×10^{-6} and 1.14×10^{-5} shown in Fig. 5, which illustrates that the HSAE method also can accurately reconstruct the microstructure of the coarse scale.

B. Rreconstruction of the 3D microstructure

The 2D reconstructions for three-phase microstructure have been performed, which demonstrates that our proposed method can generate more accurate microstructures than the SA method. A three-phase reservoir sandstone, whose corresponding coarser-scale representations are shown in Figs. 6(a)–6(c), is considered for reconstructing its corresponding 3D structure using the method introduced above. The three constituents of reservoir sandstone are clay (phase 1), pore (phase 2), and grain (phase 3), and three independent two-point correlation functions (P_{11}, P_{12}, and P_{22}) are chosen for the reconstruction of three-phase microstructure.

The proposed reconstruction method, starting with a coarse initialization structure ($32 \times 32 \times 32$), is shown in Fig. 6. For the finer-scale reconstruction shown in Fig. 6, only the corroded structural pixels (red pixels) that are present on the interface between different pixel regions participate in the finer-scale reconstruction. The finally reconstructed structures shown in Figs. 6(d) and 6(i), which exhibit the phase distribution for the computer-generated three-phase microstructure with a 4.8% volume fraction of clay, 32.5% of pore, and 62.7% of grain, own $128 \times 128 \times 128$ pixels. The three independent two-point correlation functions are compared with the original reservoir sandstone image shown in Fig. 7. The

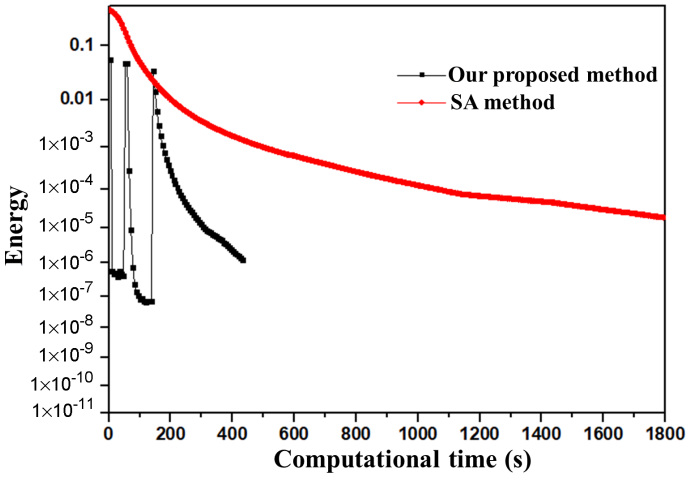

FIG. 8. Energy vs computational time (on a HP 348 G7 computer with 1.60 GHz Intel core i5 class machine): the comparison of 3D reconstruction for HSAE and SA methods.

results show that the method adopted here can reproduce microstructures with the same statistical information based on two-point statistics in a 3D microstructure.

The main advantage of the proposed method is the reduction of the computational time in the process of reconstruction. The comparison of the reconstruction energy vs computational time between the SA and HSAE methods is shown in Fig. 8, where the energy of the hierarchical annealing decreases rapidly and the final reconstruction energy of our proposed method is converged lower than that of simulated annealing. The energy curve of our proposed method has sharp peaks, which is because the fine-scale initial structure is first synthesized from the reconstructed coarse-scale structure and then eroded by structural elements, resulting in local configurations in the high-energy states. Since these high energies are due to local errors or inconsistencies, they can be easily corrected, and the energy drops immediately as the sampling algorithm progresses. As can be seen from Fig. 8, the final reconstruction time of the HSAE method is an order of magnitude faster than that of the SA method.

V. CONCLUSION

In this paper, a hierarchical annealing of erosion method is proposed to reconstruct the three-phase microstructure, which can improve the computational efficiency of reconstruction. In the reconstruction of three-phase microstructure, the two-point correlation function is chosen as the morphological descriptor and three independent two-point correlation functions are needed.

In this work, the 2D reconstructions of sandstones are carried out first. Experimental results show that the phase distribution of the reconstructed image for our proposed method is more similar to that of the original image than SA reconstruction. By comparing the two-point clustering function between the reconstructed image and the reference image, it is shown that the proposed method can generate more morphological information similar to the original image and improve the accuracy of reconstruction. Next, the 3D reconstruction of a three-phase microstructure is performed, where the two-point correlation functions of the reconstruction 3D microstructure are in excellent agreement with that of the original 2D image. This illustrates that our proposed method is effective for the reconstruction of 3D microstructure. The energy and computational time of the SA method and the HSAE method are compared, which shows that our method is an order of magnitude faster than the SA method. That is because only some of the pixels are needed to be considered for sampling in our proposed method.

ACKNOWLEDGMENTS

This work was supported by Natural Science Foundation of Henan Province (Grant No. 212300410302), Young Teacher Foundation of Henan Province (Grant No. 2021GGJS093), Science and Technology Planning Program of Henan Province (Grants No. 212102210082 and No. 20A520042), GuangXi Project of technology base and special talent (Grant No. AD19110022), Basic Ability Improvement Project of Young and Middle-Aged Teachers in Guangxi Colleges and Universities (Grant No. 2018KY0202), and GuangXi Natural Science Foundation (Grant No. 2020GXNSFAA297186).

[1] A. Bhaduri, A. Gupta, A. Olivier, and L. G. Brady, An efficient optimization based microstructure reconstruction approach with multiple loss functions, Comput. Mater. Sci. **199**, 110709 (2021).

[2] E. Patelli and G. Schuëller, On optimization techniques to reconstruct microstructures of random heterogeneous media, Comput. Mater. Sci. **45**, 536 (2009).

[3] D. D. Chen, X. H. He, Q. Z. Teng, Z. Xu, and Z. J. Li, Reconstruction of multiphase microstructure based on statistical descriptors, Phys. A (Amsterdam) **415**, 240 (2014).

[4] M. Groeber, S. Ghosh, M. D. Uchic, and D. M. Dimiduk, A framework for automated analysis and simulation of 3D polycrystalline microstructures: Part 1: Statistical characterization, Acta Mater. **56**, 1257 (2008).

[5] A. Haghverdi, M. Baniassadi, M. Baghani, A. A. Sahraei, H. Garmestani, and M. Safdari, A modified simulated annealing algorithm for hybrid statistical reconstruction of heterogeneous microstructures, Comput. Mater. Sci. **197**, 110636 (2021).

[6] D. S. Li, M. A. Tschopp, M. Khaleel, and X. Sun, Comparison of reconstructed spatial microstructure images using different statistical descriptors, Comput. Mater. Sci. **51**, 437 (2012).

[7] Y. Gao, Y. Jiao, and Y. M. Liu, Ultra-efficient reconstruction of 3D microstructure and distribution of properties of random heterogeneous materials containing multiple phases, Acta Mater. **204**, 116526 (2020).

[8] H. Xu, D. A. Dikin, C. Burkhart, and W. Chen, Descriptor-based methodology for statistical characterization and 3D reconstruction of microstructural materials, Comput. Mater. Sci. **85**, 206 (2014).

[9] A. Belvin, R. Burrell, A. Gokhale, N. Thadhani, and H. Garmestani, Application of two-point probability distribution

functions to predict properties of heterogeneous two-phase materials, Mater. Charact. **60**, 1055 (2009).

[10] A. Pommerening and D. Stoyan, Reconstructing spatial tree point patterns from nearest neighbour summary statistics measured in small subwindows, Can. J. For. Res. **38**, 1110 (2008).

[11] V. V. Novikov and D. Y. Zubkov, Fractal character of effective Hall properties of a three-dimensional disordered composite, Phys. B (Amsterdam) **400**, 6 (2007).

[12] A. C. Kak and M. Slaney, Principles of computerized tomographic imaging, Med. Phys. **29**, 107 (2002).

[13] C. J. Gommes, Three-dimensional reconstruction of liquid phases in disordered mesopores using *in situ* small-angle scattering, J. Appl. Crystallogr. **46**, 493 (2013).

[14] C. Garcia-Mateo, J. A. Jimenez, B. Lopez-Ezquerra, R. Rementeria, L. Morales-Rivas, M. Kuntz, and F. G. Caballero, Analyzing the scale of the bainitic ferrite plates by XRD, SEM, and TEM, Mater. Charact. **122**, 83 (2016).

[15] A. Viani, K. Sotiriadis, A. Len, P. Šašek, and R. Ševčík, Assessment of firing conditions in old fired-clay bricks: The contribution of x-ray powder diffraction with the Rietveld method and small angle neutron scattering, Mater. Charact. **116**, 33 (2016).

[16] P. E. Chen, W. X. Xu, N. Chawla, Y. Ren, and Y. Jiao, Hierarchical *n*-point polytope functions for quantitative representation of complex heterogeneous materials and microstructural evolution, Acta Mater. **179**, 317 (2019).

[17] P. E. Chen, W. X. Xu, Y. Ren, and Y. Jiao, Probing information content of hierarchical *n*-point polytope functions for quantifying and reconstructing disordered systems, Phys. Rev. E **102**, 013305 (2020).

[18] P. Tahmasebi and M. Sahimi, Reconstruction of three-dimensional porous media using a single thin section, Phys. Rev. E **85**, 066709 (2012).

[19] M. Baniassadi, H. Garmestani, D. S. Li, S. Ahzi, M. Khaleel, and X. Sun, Three-phase solid oxide fuel cell anode microstructure realization using two-point correlation functions, Acta Mater. **59**, 30 (2011).

[20] C. L. Y. Yeong and S. Torquato, Reconstructing random media. II. Three-dimensional media from two-dimensional cuts, Phys. Rev. E **58**, 224 (1998).

[21] P. E. Øren and S. Bakke, Reconstruction of Berea sandstone and pore-scale modelling of wettability effects, J. Pet. Sci. Eng. **39**, 177 (2003).

[22] L. Lemmens, B. Rogiers, D. Jacques, M. Huysmans, and E. Laloy, Nested multiresolution hierarchical simulated annealing algorithm for porous media reconstruction, Phys. Rev. E **100**, 053316 (2019).

[23] L. M. Pant, S. K. Mitra, and M. Secanell, Multigrid hierarchical simulated annealing method for reconstructing heterogeneous media, Phys. Rev. E **92**, 063303 (2015).

[24] S. K. Alexander, P. Fieguth, M. A. Ioannidis, and E. R. Vrscay, Hierarchical annealing for synthesis of binary images, Math. Geosci. **41**, 357 (2009).

[25] M. Teubner, Level surfaces of Gaussian random-fields and microemulsions, Europhys. Lett. **14**, 403 (1991).

[26] A. P. Roberts and M. A. Knackstedt, Structure-property correlations in model composite materials, Phys. Rev. E **54**, 2313 (1996).

[27] J. F. Thovert, F. Yousefian, P. Spanne, C. G. Jacquin, and P. M. Adler, Grain reconstruction of porous media: Application to a low-porosity Fontainebleau sandstone, Phys. Rev. E **63**, 061307 (2001).

[28] M. G. Rozman and M. Utz, Uniqueness of Reconstruction of Multiphase Morphologies from Two-Point Correlation Functions, Phys. Rev. Lett. **89**, 135501 (2002).

[29] M. A. Davis, S. D. C. Walsh, and M. O. Saar, Statistically reconstructing continuous isotropic and anisotropic two-phase media while preserving macroscopic material properties, Phys. Rev. E **83**, 026706 (2011).

[30] Y. Jiao, F. H. Stillinger, and S. Torquato, Modeling heterogeneous materials via two-point correlation functions. II. Algorithmic details and applications, Phys. Rev. E **77**, 031135 (2008).

[31] P. Capek, On the importance of simulated annealing algorithms for stochastic reconstruction constrained by low-order microstructural descriptors, Transp. Porous Media **125**, 59 (2018).

[32] Y. Jiao, F. H. Stillinger, and S. Torquato, A superior descriptor of random textures and its predictive capacity, Proc. Natl. Acad. Sci. USA **106**, 17634 (2009).

[33] C. J. Gommes, Y. Jiao, and S. Torquato, Microstructural degeneracy associated with a two-point correlation function and its information content, Phys. Rev. E **85**, 051140 (2012).

[34] C. E. Zachary and S. Torquato, Improved reconstructions of random media using dilation and erosion processes, Phys. Rev. E **84**, 056102 (2011).

[35] Y. Jiao, F. H. Stillinger, and S. Torquato, Geometrical ambiguity of pair statistics: Point configurations, Phys. Rev. E **81**, 011105 (2010).

[36] Y. Jiao, F. H. Stillinger, and S. Torquato, Geometrical ambiguity of pair statistics. II. Heterogeneous media, Phys. Rev. E **82**, 011106 (2010).

[37] C. J. Gommes, Y. Jiao, and S. Torquato, Density of States for a Specified Correlation Function and the Energy Landscape, Phys. Rev. Lett. **108**, 080601 (2012).

[38] A. N. Diógenes, L. O. E. dos Santos, C. P. Fernandes, A. C. Moreira, and C. R. Apolloni, Porous media microstructure reconstruction using pixel-based and object-based simulated annealing-comparison with other reconstruction methods, Therm. Eng. **8**, 35 (2009).

[39] T. Tang, Q. Z. Teng, X. H. He, and D. S. Luo, A pixel selection rule based on the number of different-phase neighbours for the simulated annealing reconstruction of sandstone microstructure, J. Microsc. **234**, 262 (2009).

[40] D. D. Chen, Q. Z. Teng, X. H. He, Z. Xu, and Z. J. Li, Stable-phase method for hierarchical annealing in the reconstruction of porous media images, Phys. Rev. E **89**, 013305 (2014).